Absolute Measurement of Surface-Vibration-Patterns in Piezoelectric Devices Using Two Lasers with Different Wavelengths

Yasuaki Watanabe, Noriyuki Imaeda, Shigeyoshi Goka,
Takayuki Sato and Hitoshi Sekimoto
Graduate School of Science and Engineering
Tokyo Metropolitan University
Tokyo 192-0397, Japan
y.watanabe@ieee.org

Sunao Ishii
Hitachi, Ltd.
Information and Communication Group,
Tokyo 100-8280, Japan

Abstract— **Our new method solves the limitation of the previous measurement system for in-plane vibration displacement, using two semiconductor lasers with adequately separated wavelengths. Different γs, that is, interference factors, are determined for each speckle image by using lasers with different wavelengths. The ratio of the two γs is proportional to the reciprocal of the wavelength ratio of the lasers. The distributions of the absolute vibration displacement can be mapped based on this relationship and statistical processing of the speckle images. A red laser and a violet laser were used in the actual measurement system. A 23-MHz circular AT-cut quartz resonator was used to test the validity of our method, and the results are compared here to the results previously obtained by the two-drive-level burst wave excitation method. Our experiments showed good agreement between the two displacements, thereby validating the proposed method.**

I. INTRODUCTION

A number of methods for plotting the mode shapes of piezoelectric resonators have been developed. Measuring the vibration mode shape is very important when designing resonators or vibration devices. Many of these methods use optical interference, which is the interaction between incident and reflected photons produced by coherent laser beams [1].

The laser speckle method, which uses the long coherence of modern lasers, is a powerful tool for visualizing shape displacement and has led to the development of many visualizing techniques [2-6]. Since the speckle pattern is very sensitive to changes in path length, this method can be applied to piezoelectric resonators with minute displacements.

High-frequency piezoelectric resonators are generally small, and their surfaces are not sufficiently rough to use classical laser speckle methods directly. We have therefore developed three methods for visualizing mode shapes that combine surface speckle interferometry and image-processing techniques for high-frequency resonators [7-9]. The methods all use a process that involves irradiating the surface of a roughly finished device with a collimated laser beam and capturing images of the speckle field generated on the surface with a video camera. The mode shapes are then obtained from the correlation between images taken during the resonator's resting and driving states. We improved this method to apply it to piezoelectric devices with polished surfaces [10].

We previously reported an improved laser speckle method that increases detection sensitivity using stroboscopic laser irradiation and estimates the absolute vibration displacement [11-13]. This method was based on a simple surface-interferometric model and statistical operations for the interference intensity of the speckle images.

We also developed a burst-wave driving laser speckle system[14]. Although this system consists of very simple optics and electrical equipment and can be used with very-high-frequency devices, it requires two measurements with different device driving levels. This requirement limits the application of the system to devices with minute vibration displacements or with nonlinear characteristics.

In this paper, we explain how our new method solves the limitation using two semiconductor lasers with adequately separated wavelengths. We used the relationship between the interference factors, γs, of speckle images and the wavelengths of laser diodes to avoid the two-level device excitations of the previous burst-wave driving system.

A red laser (λ = 655 nm) and a violet laser (λ = 405 nm) were used in the actual measurement system. The distributions of the absolute vibration displacement can be mapped based on this relationship and on the statistical processing of the speckle images using two lasers. The experimental results obtained using the proposed method show good agreement with the previous results obtained using the burst excitation method.

1-4244-0647-1/07/$20.00 ©2007 IEEE

II. MEASUREMENT PRINCIPLE

Generally, interferometric intensity is given by the following equation when the laser beam is parallel to the resonator surface[15].

$$I = \bar{I}_0 + \gamma \cos 2kdx \qquad (1)$$

Here, $k = 2\pi/\lambda$, λ is the wavelength of the laser diode, $\overline{I_0}$ is the average intensity of the interference, γ is the interference factor of the fringes, and dx is the vibration displacement of the resonator. Interference factor γ is affected by the surface conditions of the resonator and the optical construction of the measurement system.

In the burst-wave excitation system, the difference in speckle brightness caused by the interference condition between the resonator's resting and driving states is approximately given by transforming and integrating Equation 1 as

$$\Delta I = \gamma\left(1 - \frac{\sin 2kdx}{2kdx}\right). \qquad (2)$$

In this equation, we assume that dx changes linearly and is relatively large. Although dx on the surface of actual piezoelectric resonators changes sinusoidally, we daringly used a simple approximation because interference patterns spread randomly, making mathematical treatment for the speckle field quite complicated.

We can easily understand from the equation that γ is not explicitly obtained by changing dx as a parameter. Therefore, we used a second-order polynomial function to approximate Equation 2. The second term in the parentheses in Equation 2 can be formally expressed as

$$\frac{\sin 2kdx}{2kdx} \cong \alpha dx^2 + \beta dx + 1, \qquad (3)$$

where α and β are negative constants and can be derived by determining λ and the approximation range. If Equation 3 is complete, we cannot derive dx because β becomes zero. However, by limiting the measurement range to a large displacement region as discussed above, β is not set to zero. Thus, we can use the following relationship and estimate dx.

In the following treatments, we assumed that γ is reciprocally proportional to the wavelength of the laser in the speckle interference field. We show the validity of this assumption from the experimental results.

By rearranging Equation 3, differences in brightness in the kernels for each laser, ΔI_1 and ΔI_2, can be obtained by

$$\begin{cases} \Delta I_1 = -\gamma(\alpha_1 dx^2 + \beta_1 dx) \\ \Delta I_2 = -p\gamma(\alpha_2 dx^2 + \beta_2 dx) \end{cases}, \qquad (4)$$

where p is the ratio of the wavelength of the lasers, given by $p=\lambda_1/\lambda_2$. The interference factor γ can be obtained by solving Equation 5.

$$\gamma = -\frac{\left(\alpha_2 \Delta I_1 - \frac{\alpha_1}{p}\Delta I_2\right)^2}{(\alpha_1\beta_2 - \beta_1\alpha_2)\left(\beta_2 \Delta I_1 - \frac{\beta_1}{p}\Delta I_2\right)}, \qquad (5)$$

We can thus obtain the absolute vibration amplitude dx of the in-plane vibration using Equation 6.

$$dx = \frac{-\beta_1 - \sqrt{\beta_1^2 - 4\alpha_1 \Delta I_1/\gamma}}{2\alpha_1}. \qquad (6)$$

A practical approach follows.

1) *Measure all images: (Images 1_0 (resting) and 1_1 (driving) using LD_1; Images 2_0 and 2_1 using LD_2; Residual noise images for each LD.)*
2) *Calculate the mode shape and contour map using a two-dimensional correlation function for Image 1_0 and Image 1_1.*
3) *Divide the set of image areas that has approximately the same vibration amplitude.*
4) *Re-divide the above areas into 5×5 pixels.*
5) *Find the pair of pixels that gives the maximum optical intensity difference in the re-divided areas.*
6) *Map the frequency distribution characteristics of the maximum intensity differences in the divided area with the same vibration amplitude to find representative optical intensity difference ΔI_n.*
7) *Repeat step 5) for "Image 2" to obtain ΔI_2.*
8) *Subtract ε (=ΔI_0 for each LD) from ΔI_1 and ΔI_2 to cancel environmental noise.*
9) *Calculate interference factor γ using Equation 5 and representative displacement dx in the area by Equation 6.*
10) *Repeat step 5) for all divided areas.*

III. MEASUREMENT METHOD

Figure 1 is a block diagram of the measurement system using two LDs and burst wave device driving. In this system, a mirror is placed on the opposite side of the laser. This optical system enhances the interference intensity of the sample surface when the in-plane vibration displacement is measured. The incident angle of the laser in the system used was set to 10 degrees from the sample surface. We previously reported that this angle can be taken as zero from the experimental results [16]. To avoid a polarization error in the optical parts such as the half-mirror, the measurement was carried out by interchanging the LDs keeping the same incident angle.

The resonator is driven by a signal generator (SG), and the driving signal is tuned to the resonant frequency and pulse-modulated by the output of a low-frequency oscillator (LFO). A charge-coupled device (CCD) color video camera was used to capture the diffusion light component on the surface of the sample. The vibration patterns were obtained as reciprocals of the correlation coefficients between the images for the resting and driving states. The above-mentioned LDs with linear polarization generate visible range beams, and their optical powers and wavelengths were 10 mW and 655 nm for the red LD and 30 mW and 405 nm for the violet LD, respectively.

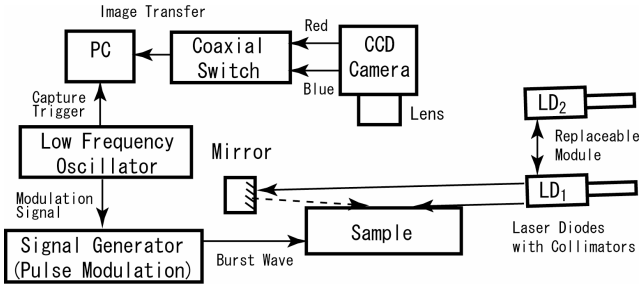

Figure 1. Experimental setup of full-field in-plane motion visualization system using burst resonator excitation.

The maximum spatial resolution and dynamic range of the CCD had 640×480 pixels and 48 dB (256:1) due to the use of an 8-bit camera. The red and blue components of the images are captured separately. Although the CCD video camera has different brightness sensitivities for each color component, the burst device driving method effectively cancels this sensitivity difference that affects the absolute measurement of the surface vibration displacement.

Since the difference in brightness caused by the interference between two images, i.e., from the resonator resting state and resonator driving state, is lower than the lowest brightness resolution of the CCD, individual pairs of images were accumulated in order to improve the detection sensitivity and noise reduction. The size of the images was reduced to 256×256 pixels to reduce the data-transfer and calculation time. The kernel for calculating the correlation between the two accumulated images consisted of 5×5 pixels, which was sufficiently smaller than the wavelength of the acoustic wave on the resonator surface.

IV. Results

We used a 23-MHz circular fundamental AT-cut quartz resonator with a roughly finished surface (#4000) with partial electrodes. The target area was set near the center of the electrode where the maximum in-plane vibration displacement is observed in its fundamental thickness shear mode.

A. Characteristics of interference factor for laser wavelength and resonator driving level

To confirm that interference factor γ is reciprocally proportional to the wavelength of the laser in the speckle interference field, we measured γs using the two-driving-level method[14] with red and blue lasers, and calculated the ratio of the two γs. We also measured the vibration level dependency of γ by changing the resonator driving level.

Figure 2 plots the measurement results. The ordinate axis indicates γ and the abscissa axis is the resonator driving level at the output of the signal generator. The averaged results using red (λ = 655 nm) and violet (λ = 405 nm) lasers are indicated by filled and open circles, respectively. Experiments were repeated five times each.

The ratios of γs for each laser at the resonator drive level of +6 and +8 dBm were 0.620 and 0.608, respectively. The reciprocal ratio of the laser wavelengths was 0.618 and agreed with the experimental results within an error of 1.7%. These results show that γ is reciprocally proportional to the ratio of laser wavelengths even in the speckle interference field; that is, the assumption of Equation 4 is correct. The drive level dependency of 1.2%/dB is also negligible for practical use.

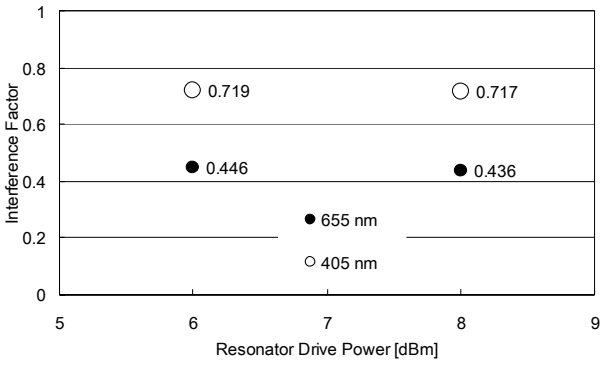

Figure 2. Power dependence of interference factor γ for two wavelengths (λ = 655 nm and 405 nm).

B. Absolute measurement of vibration displacement

Figure 3 plots the experimental results using the proposed method and the two-level burst-wave driving laser speckle method[14] with red and violet lasers. The results using the burst-wave driving laser speckle system has been confirmed by an absolute estimation system[13] for in-plane vibration displacement. The number of measurements taken to obtain a data average was 200 each. The open circles and open squares respectively represent the measured in-plane displacement using the burst-wave driving laser speckle system with red and violet lasers. The filled circles indicate the measured in-plane displacement using the proposed method.

The experimental results for the burst-wave driving laser speckle system and the proposed system agree within 30 nm when the resonator driving level is + 6 dB. However, the results using the burst-wave driving laser speckle system with the violet laser disagree with the results of the other methods.

This disagreement is due to the large vibration displacement compared to the wavelength of the violet laser.

C. *In-plane mode shape measurement of entire electrode area*

Figure 4 shows the mode shape of the fundamental thickness shear mode on the surface of the same AT-cut quartz resonator. An absolute scale for the amplitude of in-plane vibration displacement and the orientation of the quartz resonator are also shown in the figure. The experimental conditions were the same as for the experiments described in the previous subsection. The resonator driving level was + 6 dBm of the signal generator (SG) output level. The white spots on the image are dust particles that are sticking to the surface. The dust particles attract large scattering and cause saturation of the CCD video camera. Thus, the white spots are classified as nonmoving parts. This figure demonstrates that the vibration amplitude is trapped in the midsection of the electrode area.

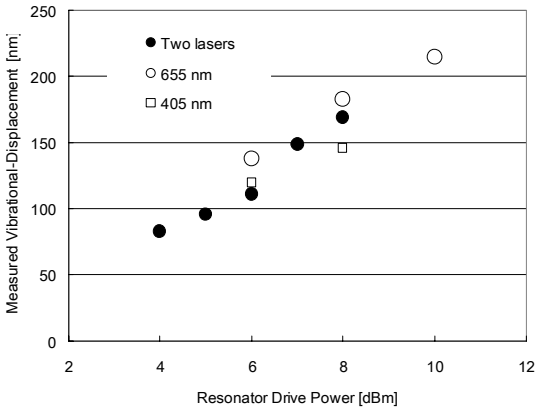

Figure 3. Experimental results of proposed method and two-level burst driving method with red and violet lasers.

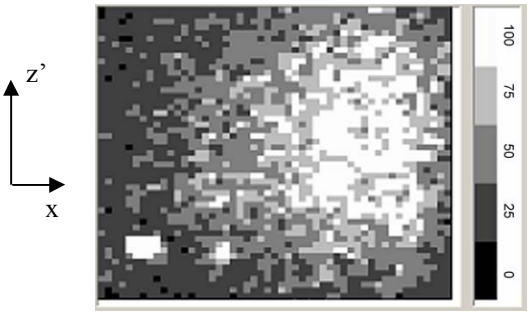

Figure 4. Experimental results for 23-MHz circular AT-cut quartz resonator. (N=200; drive level = +6 dBm).

The in-plane vibration displacement was approximately 100 nm in the midsection and is reasonable for the resonator driving level. Although areas of vibration amplitude below 50 nm are also indicated in the figure, these values are extrapolated data using the results over 75 nm.

V. CONCLUSIONS

We have developed a full-field absolute vibration displacement imaging method that is based on two lasers with different wavelengths and single-level burst-wave resonator driving. We confirmed that the ratio of interference factor γs for each laser wavelength is reciprocally proportional to the laser wavelengths even in the speckle interference field. The reliability of the proposed method was confirmed by comparing the experimental data to those of the two-level burst driving method. We also used the method to measure the entire electrode area in a quartz resonator.

Although two series of measurements were carried out for the two lasers in these experiments, the system will be improved to allow simultaneous measurement with two lasers using a dedicated optical system.

REFERENCES

[1] R. J. Williamson: Proc. 44th Annu. Symp. Freq. Control, 1990, pp. 424.

[2] H. J. Tizianni: Optica Acta **18** (1971) 891.

[3] D. E. Duffy: Appl. Opt. **11** (1972) 1778.

[4] J. Monchalin: IEEE Trans. Ultrason. Ferroelectr. and Freq. Control 35 (1986) 485.

[5] W. Wang, C. Hwang and S. Lin: Appl. Opt. **35** (1996) 4502.

[6] C. Ma and C. Huang: IEEE Trans. Ultrason. Ferroelectr. and Freq. Control **48** (2001) 142.

[7] Y. Watanabe, Y. Shikama, S. Goka, T. Sato and H. Sekimoto: Jpn. J. Appl. Phys. **40** (2001) 3572.

[8] Y. Watanabe, T. Tominaga, T. Sato, S. Goka and H. Sekimoto: Jpn. J. Appl. Phys. **41** (2002) 3313.

[9] Y. Watanabe, T. Sato, S. Goka and H. Sekimoto: Proc. IEEE Ultrasonic Symp., 2002, pp. 928.

[10] Y. Watanabe, S. Goka, T. Sato and H. Sekimoto: IEEE Trans. Ultrason. Ferroelectr. and Freq. Control **51** (2004) 491.

[11] Y. Watanabe, K. Tsuno, T. Tsuda, S. Goka, T. Sato and H. Sekimoto: Proc. 2004 Annu. Symp. Freq. Control, 2004, pp. 591.

[12] Y. Watanabe, K. Tsuno, T. Tsuda, S. Goka and H. Sekimoto: Jpn. J. Appl. Phys. **44** (2005) 4440.

[13] Y. Watanabe, T. Tsuda, S. Ishii, S. Goka and H. Sekimoto: Jpn. J. Appl. Phys. **45** (2006) 4585.

[14] Y. Watanabe, S. Ishii, S. Goka, H. Sekimoto, M. Kato and T. Tsuda: Proc. 2006 Annu. Symp. Freq. Control, 2006, pp.554

[15] Y. Watanabe, H. Kitabori, S. Goka, T. Sato and H. Sekimoto: Trans on IEICE, **J86-C** (2003) 1337.

[16] Y. Watanabe, T. Sato, S. Goka and H. Sekimoto: Acoust. Sci. & Tech. **23** (2002) 284.